

Silicon-based integrated interferometer with phase modulation driven by surface acoustic waves

Christophe Gorecki, Franck Chollet, Eric Bonnotte, and Hideki Kawakatsu

Laboratory for Integrated Micro-Mecatronic Systems/Centre National de la Recherche Scientifique,
Institute of Industrial Science, University of Tokyo, 7-22-1 Roppongi, Minato-ku, Tokyo 106, Japan

Received July 15, 1997

As a novel application of silicon-based integrated optics, results from a proposed compact Mach-Zehnder interferometer are presented. The deposition of a ZnO thin-film transducer upon the reference arm of the interferometer transforms this optically passive device into a device with active sinusoidal phase modulation. © 1997 Optical Society of America

Three main physical effects are used for generation of phase modulation in thin-film optical waveguides: electro-optic, thermo-optic, and acousto-optic.¹ Phase modulators consist of a dielectric waveguide and an appropriate electrode structure. The structure of these devices can be classified into one of two generic categories: (i) the substrate upon which the optical waveguide is constructed is a piezoelectric material or (ii) the substrate is a nonpiezoelectric material.² The electro-optic effect, which permits operation of devices in category (i), offers efficient modulation to a 10-GHz frequency range but is restricted to piezoelectric substrates such as LiNbO₃, LiTaO₃, and GaAs, which have large Pockels coefficients. Since microelectromechanical systems must be constructed upon silicon-based substrates, fabrication of modulators upon nonpiezoelectric substrates is attractive.³ Thermo-optic and acousto-optic effects in principle permit operation in category (i). The thermo-optic effect is limited to the kilohertz range, however. The acousto-optic effect with surface acoustic waves (SAW's) as proposed here can be used for modulators in the megahertz range. To obtain a device with active phase modulation, we generated a SAW by means of a thin-film piezoelectric transducer deposited near the silicon-based optical waveguide. The resulting acousto-optic interaction mechanism is based on the change in the index of refraction caused by mechanical strain that is introduced by the passage of an acoustic wave.^{4,5} An optical spectrum analyzer using this modulation technique, working to a 1-GHz frequency range, was reported in Ref. 3.

The proposed Mach-Zehnder interferometer architecture shown in Fig. 1 (Ref. 6) consists of combined measuring and reference arms composed of two symmetrical Y junctions integrated upon a silicon substrate. Phase modulation is obtained when the guided reference beam is passed through a SAW generated on a ZnO thin-film transducer driven by an interdigital electrode structure. ZnO has a low dielectric constant and a high electromechanical coupling factor, making it an interesting material for SAW devices. To avoid perturbations of the measuring arm of the interferometer, one must confine acoustic waves to the region of the reference arm by means of an isolation trench.

For our specific application a single-mode strip-load silicon oxinitride (SiON) waveguide operating at a wavelength of 660 nm is preferred (Fig. 2). The waveguide core was a SiON thin film of 0.5 μm sandwiched between two SiO₂ layers deposited by low-pressure chemical-vapor deposition upon a silicon substrate. The SiON layer was fabricated with a refractive index $n = 1.51$ at a temperature of 850 °C by adjustment of the flow of SiH₄-N₂O-NH₃ reactant gases at a pressure near 0.4 Torr. The deposition rate of this reaction was 3 nm/min. SiO₂ layers with a refractive index $n = 1.454$ were deposited at a temperature of 600 °C by adjustment of the SiH₄-O₂ mixture in a pressure range of 0.3 Torr. The deposition rate was 30 nm/min. By means of reactive ion etching in a CHF₃ plasma, a 4- μm -wide rib was etched upon the top SiO₂ layer. This overlayer structure laterally confined the optical field. The obtained etch rate was 30 nm/min. We calculated the field distribution in the output cross section for a Mach-Zehnder interferometer with a total length of 24 mm and a gap of 400 μm between the measuring and the reference arms with the three-dimensional beam-propagation method, as shown in Fig. 3. The result confirms the excellent confinement of the optical field for the above-described structure and permits visualization of the lateral size of the guided mode. The deposition condition for generation of SAW's was obtained when the c axis of the ZnO layer was perpendicular to the substrate, with a spread of 0–5°. We fabricated a 2.5- μm -thick ZnO film by rf diode sputtering in an 80% argon–20%

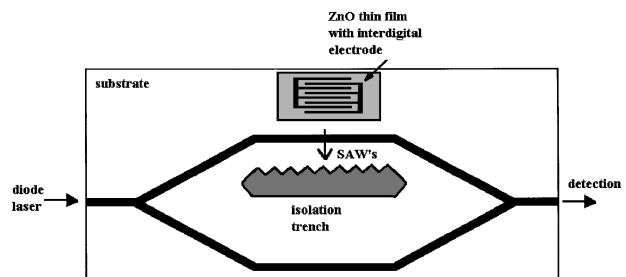


Fig. 1. Schematic diagram of the Mach-Zehnder interferometer architecture.

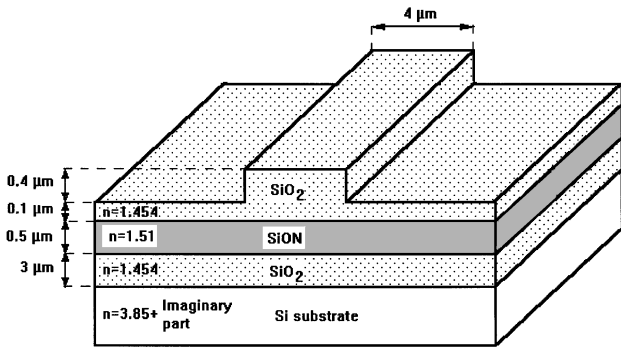


Fig. 2. Structure of the SiO_2 - SiON - SiO_2 strip-load waveguide.

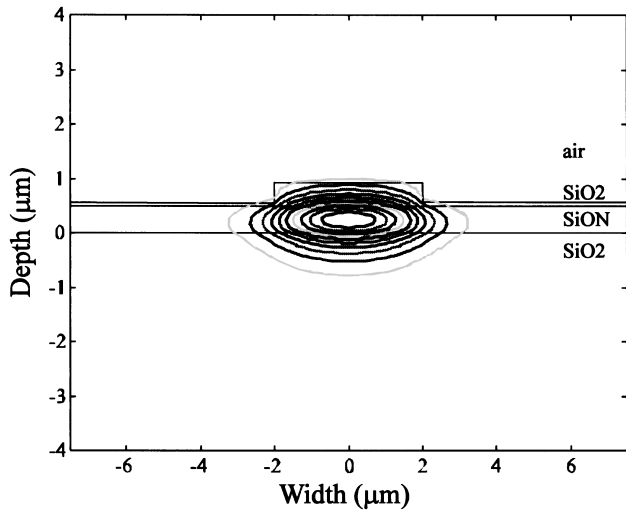


Fig. 3. Optical field distribution of a single-mode strip-load waveguide ($\lambda = 660 \text{ nm}$) calculated by use of the beam-propagation method.

oxygen atmosphere. At a temperature of 250°C the film-deposition rate was 16 nm/min . To fabricate the interdigital electrode we deposited a thin film of Al upon the top surface of the ZnO layer by vacuum evaporation. The metal layer was subsequently wet etched for patterning of the structure of the transducer electrode. The distance between the transducer and the waveguide was 0.3 mm . To pattern the isolation trench, we used deep reactive ion etching. Figure 4a represents a scanning electron microscope photograph of one of the Y junctions just after the patterning of the SiO_2 rib, and Fig. 4b shows the structure of the transducer electrode.

For an N -period interdigital transducer the frequency variation of the acoustic amplitude can be approximated for frequencies near ω_0 by the function $\sin x/x$, where $x = N\pi(\omega - \omega_0)/\omega_0$. A useful criterion for transducer performance is the transducer quality factor, defined as^{7,8}

$$\frac{1}{Q} = \omega_0 N C_s R_A = N \pi \frac{\Delta \nu}{\nu} = \frac{\pi}{2} N k^2, \quad k^2 = 2 \left(\frac{\Delta \nu}{\nu} \right), \quad (1)$$

where ω_0 is the center-of-band frequency, C_s is the elementary finger capacitance, k^2 is the electromechanical coupling coefficient, R_A is the radiation impedance,

and $\Delta \nu$ is the change in acoustic velocity caused by introduction of a short-circuiting plane into the plane of the interdigital electrode.

Under the condition of the matching network defined by Smith *et al.*⁷ the electronic bandwidth of the system is determined by the product $\Delta \nu/\nu$ and the number N of finger pairs. Q is then proportional to $1/N$ when the optimum value of N is used. Our transducer has an interdigital period of $60 \mu\text{m}$ (this corresponds to a frequency of $f_0 = 48 \text{ MHz}$) with a finger width of $15 \mu\text{m}$ and an electrode aperture width of $L = 5.8 \text{ mm}$. When $R_A = 75 \Omega$ and $C_s = 0.14 \text{ pF}$, the transducer with $N = 15$ is found to have the optimum fractional bandwidth of 0.08, which corresponds to a 3-dB conversion loss ($1/N = 0.067$). We evaluated the bandwidth characteristics of the transducer by measuring the conversion loss of a delay line composed of two identical interdigital electrodes placed one after the other, with a spacing between the input and output transducers of 7 mm , giving a delay of approximately $2.2 \mu\text{s}$. This delay line was connected to a source generator with an impedance of 50Ω . Figure 5 shows a comparison of calculated and measured conversion losses for this delay line, plotted as a function of frequency, for a $2.5\text{-}\mu\text{m}$ ZnO film. The conversion loss is defined as $\text{CL} = 10 \log(P_S/P_{IN})$, where P_S is maximum power available from the generator source and P_{IN} is the power absorbed inside the delay line.

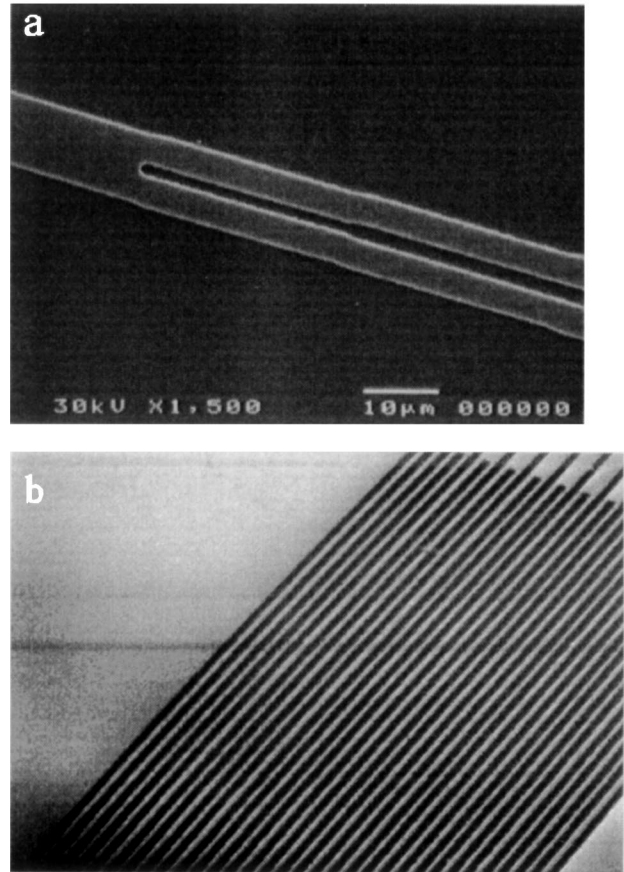


Fig. 4. Scanning electron microscope photographs of structures: a, Y junction with a $4\text{-}\mu\text{m}$ rib; b, Al interdigital electrode.

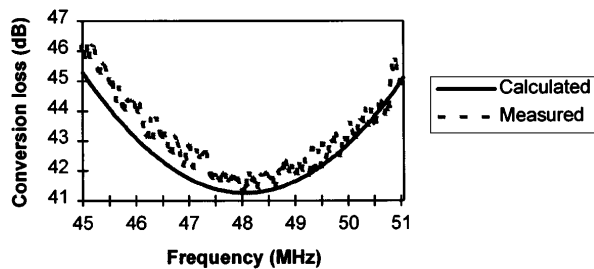


Fig. 5. Comparison of theoretical (calculated) and measured conversion losses for a delay line with a 15-finger-pair transducer.

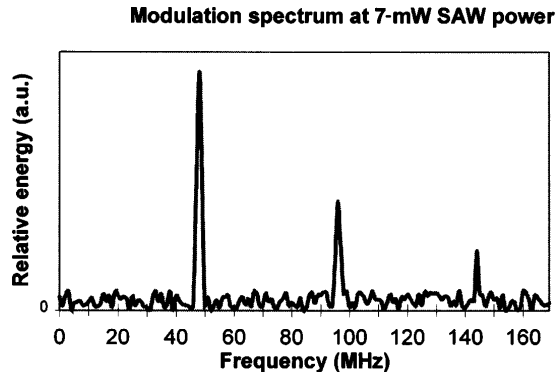


Fig. 6. Measured modulation spectrum at 7-mW SAW power.

In practice the measuring procedure consisted of detecting power variations between two transducers. As one can see there is good agreement of the measurement with the theoretical response.

To evaluate the optical performance, we coupled a diode laser beam operating at 660 nm into the waveguide via a microscope objective lens. The strip-load waveguide loss as measured by a cutback technique was 3 dB/cm. In this wavelength range the optical loss was lower than at the 890-nm wavelength as a result of lower absorption of the evanescent field on the silicon substrate. The maximum spot size of the guided mode, estimated to be $\sim 6.5 \mu\text{m}$ (Fig. 3), was much smaller than the SAW wavelength of $60 \mu\text{m}$. In this condition there was no diffraction, and the guided optical wave was only sinusoidally phase modulated. This phase-modulation experiment involved detecting the spectrum of the interference signal with a spectral analyzer, as shown in Fig. 6. The spectrum was obtained at a SAW drive power of $P_a = 7 \text{ mW}$ (P_a is the acoustic power over interaction width L). As expected, there is a component that is due to the SAW

frequency $f_0 = 48 \text{ MHz}$ (first harmonic). The second and third harmonics also appear at frequencies spaced by f_0 .⁹ It was possible to estimate the phase shift from the detected ratio of the first to the third harmonics. The amplitude of the third harmonic was $\sim 20 \log[J_1(\delta\varphi)/J_3(\delta\varphi)] = 31 \text{ dB}$ below the first harmonic, where J_1 and J_3 are the Bessel functions. We have $J_1(\delta\varphi)/J_3(\delta\varphi) = 36.15$, and the phase shift was determined to be $\delta\varphi = 0.8 \text{ rad}$.

In conclusion, we have developed a silicon-based microinterferometer with significant SAW phase modulation by deposition of a ZnO thin-film transducer upon the reference arm. The key reason for choosing a silicon-based multilayer waveguide is that this structure provides flexible tools for designing the best optical architecture needed for increased efficiency of acousto-optic interactions, which is also interesting in view of the compatibility of the device with microelectromechanical system technology. Improving the performance of the integrated device will require many improvements in both the optical and the acoustic fields. A future biosensor application of the device will be the measurement of the concentration of fluorescent substances in the air. In such a measurement the measuring arm of a Mach-Zehnder interferometer will be covered with a polymer layer that is sensitive to the gaseous compounds to be measured, which will modify the effective index of refraction of the structure. Measurement of effective refractive-index changes as small as 10^{-4} is expected.

The authors thank the Canon Foundation in Europe for supporting this research.

References

1. R. G. Hunsperger, *Integrated Optics: Theory and Technology* (Springer-Verlag, Berlin, 1991).
2. C. H. Von Helmolt, *J. Lightwave Technol.* **LT-5**, 218 (1987).
3. S. Valette, J. Lizet, P. Mottier, J. P. Jadot, P. Gidon, and S. Renard, *Proc. Inst. Electr. Eng. Part H* **131**, 325 (1984).
4. C. P. Sandbank and M. B. N. Butler, *Electron. Lett.* **7**, 501 (1971).
5. F. S. Hickernell, *J. Appl. Phys.* **44**, 1061 (1973).
6. C. Gorecki, F. Chollet, and H. Kawakatsu, *Proc. SPIE* **3008**, 152 (1997).
7. W. R. Smith, H. M. Gerard, J. H. Collins, T. M. Reeder, and H. J. Shaw, *IEEE Trans. Microwave Theor. Tech.* **MTT-17**, 856 (1969).
8. G. S. Kino and R. S. Wagers, *J. Appl. Phys.* **44**, 1480 (1973).
9. W. Pushert, *Opt. Commun.* **10**, 357 (1974).